Linkage Analysis of a Model Quantitative Trait in Humans: Finger Ridge Count Shows Significant Multivariate Linkage to 5q14.1

Sarah E. Medland[1,2*], Danuta Z. Loesch[3], Bogdan Mdzewski[3†], Gu Zhu[1], Grant W. Montgomery[1], Nicholas G. Martin[1]

1 Genetic Epidemiology Unit, Queensland Institute of Medical Research, Brisbane, Australia, 2 Virginia Institute of Psychiatric and Behavioral Genetics, Virginia Commonwealth University, Richmond, Virginia, United States, 3 Department of Psychological Science, La Trobe University, Melbourne, Australia

The finger ridge count (a measure of pattern size) is one of the most heritable complex traits studied in humans and has been considered a model human polygenic trait in quantitative genetic analysis. Here, we report the results of the first genome-wide linkage scan for finger ridge count in a sample of 2,114 offspring from 922 nuclear families. Both univariate linkage to the absolute ridge count (a sum of all the ridge counts on all ten fingers), and multivariate linkage analyses of the counts on individual fingers, were conducted. The multivariate analyses yielded significant linkage to 5q14.1 (Logarithm of odds [LOD] = 3.34, pointwise-empirical *p*-value = 0.00025) that was predominantly driven by linkage to the ring, index, and middle fingers. The strongest univariate linkage was to 1q42.2 (LOD = 2.04, point-wise *p*-value = 0.002, genome-wide *p*-value = 0.29). In summary, the combination of univariate and multivariate results was more informative than simple univariate analyses alone. Patterns of quantitative trait loci factor loadings consistent with developmental fields were observed, and the simple pleiotropic model underlying the absolute ridge count was not sufficient to characterize the interrelationships between the ridge counts of individual fingers.

Citation: Medland SE, Loesch DZ, Mdzewski B, Zhu G, Montgomery GW, et al. (2007) Linkage analysis of a model quantitative trait in humans: Finger ridge count shows significant multivariate linkage to 5q14.1. PLoS Genet 3(9): e165. doi:10.1371/journal.pgen.0030165

Introduction

Finger ridges and ridge patterns are highly heritable, durable, and age-independent human traits and have been studied as a model quantitative trait in humans for over 80 years [1] . They develop between approximately the 13th and 18th weeks of gestation, and in the absence of trauma remain essentially unchanged throughout life. The cutaneous mechanoreceptive afferent neurons that innervate the fingertips develop in alignment with the ridges [2], lending support to the theory that fingerprints play a role in gripping [3] and tactile perception [4]. While relatively little is known about the developmental processes underlying fingerprint patterns, these results suggest that factors influencing the direction and complexity of ridge pattern formation also influence the receptive fields of the mechanoreceptors.

The development of ridge patterns coincides with the regression of embryonic volar pads on fingers, and the type and size of patterns are largely determined by the size and timing of subsidence of these pads [5]. Any genetically or environmentally determined growth disturbances that affect the limbs in the critical period of ridge formation may also affect normal development of ridges and ridge patterns. Finger ridge count is also subject to a sex chromosome dosage effect, with the largest count encountered in females with X monosomy (Turner's syndrome) and the lowest in the X, Y polysomies [5]. Hence, dermatological traits can assist in determining the nature and timing of developmental disturbance.

Traditionally, the ridge count is defined as the number of ridges that intersect or touch the line drawn from the easily recognized triradius (where three ridges meet) to the center of the pattern [6]. The most common pattern, a simple loop (60%–70% of all patterns [6]), characterized by a single triradius, is most advantageous for tactile perception [7] and precision grip [3]. Whorls have two triradii yielding two counts, while simple arches have no true triradii, resulting in a zero count. When the ridge count is used as a measure of a maximum pattern size on fingers, only the largest count from each finger is scored, and their sum is defined as the total ridge count. Alternatively, the sum of all possible counts on all ten fingers can be calculated yielding an absolute ridge count (ARC) [5], a measure of the total pattern size.

Both total ridge counts and ARC are highly heritable. Genetic effects have been found to account for 90%–95% of the variation on these measures. Estimates using either traditional correlation-based methods [5,6] or structural equation models fitted to twin and sibling [7] or family [8–10] data have found additive genetic effects to account for around 90% of the variation. That the remaining genetic variation arises from dominance and/or higher order genetic effects was initially suggested by skewness in the distribution of these measures [6] and supported by the modeling of twin and sibling data [7].

Editor: Jonathan Marchini, University of Oxford, United Kingdom

Received May 8, 2007; **Accepted** August 8, 2007; **Published** September 28, 2007

Abbreviations: ARC, absolute ridge count; IBD, identity by descent; LOD, logarithm of odds; QTL, quantitative trait locus

* To whom correspondence should be addressed. E-mail: smedland@vcu.edu

† Bogdan Mdzewski died on 30 November 2001 and this paper is dedicated to his memory

Author Summary

Finger ridge count (an index of the size of the fingerprint pattern) has been used as a model trait for the study of human quantitative genetics for over 80 years. Here, we present the first genome-wide linkage scan for finger ridge count in a large sample of 2,114 offspring from 922 nuclear families. Our results illustrate the increase in power and information that can be gained from a multivariate linkage analysis of ridge counts of individual fingers as compared to a univariate analysis of a summary measure (absolute ridge count). The strongest evidence for linkage was seen at 5q14.1, and the pattern of loadings was consistent with a developmental field factor whose influence is greatest on the ring finger, falling off to either side, which is consistent with previous findings that heritability for ridge count is higher for the middle three fingers. We feel that the paper will be of specific methodological interest to those conducting linkage and association analyses with summary measures. In addition, given the frequency with which this phenotype is used as a didactic example in genetics courses we feel that this paper will be of interest to the general scientific community.

The ridge counts of individual fingers are interrelated (correlations range from ~0.4 to 0.8) and highly heritable, with the lowest heritability (~0.50) observed for the thumb and little fingers [5,6,8]. These findings have led to the development of a variety of models to explain the genetics of finger ridge count, the simplest of which postulates pleiotropic gene effects that assume a single genetic factor determining the general magnitude of the counts and random influences accounting for between-finger variation [6]. More complex models, such as those developed by Martin et al. [7], have found shared genetic effects common to all digits, in addition to patterns of covariation suggestive of developmental fields acting across the fetal hand, implying heterogeneous gene action between digits.

The aim of this study was to identify loci influencing finger ridge counts by conducting a genome scan on 2,114 twin and singleton offspring from 922 twin families (equivalent to 2,826 quasi-independent sib pairs). The data were collected from two twin cohorts; an adolescent sample (which included non-twin siblings) [11,12] and an adult sample [13]. As described in the Materials and Methods section below, prints were not available for digits IV and V for participants from the adult study.

Given the evidence for developmental field effects from quantitative genetic analysis, we conducted both univariate (ARC) and multivariate (simultaneously modeling ridge counts (radial + ulnar) for each of the ten fingers) variance components linkage analyses. The aim was to determine whether loci influencing ridge count acted in a simple pleiotropic fashion (i.e., all fingers were influenced by the same loci to the same extent), or if more complicated pleiotropic patterns indicative of field effects were present (e.g., a quantitative trait locus's (QTL's) maximum influence was seen on the little finger and the effects tapered off towards the thumb).

Results

As shown in Figure 1, the strongest evidence for univariate linkage for ARC was seen at 1q42.2 (250 cM, Logarithm of odds (LOD) = 2.04; point-wise p-value = .002, genome-wide p-value = .29). At this position, the QTL explained 21% of the variance in ARC, while the multivariate test revealed low QTL factor loadings across the five fingers, explaining 7.7%, 12.7%, 10.0%, 13.8%, and 9.3% of the variation in individual counts from thumb to little finger, respectively (Figure 2A). As may be expected for a locus at which small pleiotropic effects were found for all digits, the multivariate test for linkage was less powerful than the univariate test (multivariate LOD = .46), because the pattern of factor loadings is most economically summarized by the mean (or total) score with a single degree of freedom [14]. The next highest univariate LOD scores were found at 15q26.1 (95cM, LOD = 1.52; point-wise p-value = .006, genome-wide p-value = .62) and 7p15.3 (35cM, LOD= 1.26; point-wise p-value = .01, genome-wide p-value = .79). Loci with LOD scores greater than 1 are listed in Table 1.

The strongest evidence for multivariate linkage was seen at 5q14.1 (95 cM, multivariate LOD = 3.34). As shown in Figure 2B, the pattern of loadings is consistent with a developmental field factor whose influence is greatest on the ring finger, falling off to either side. It is interesting that the highest heritability for ridge count is seen for the middle three

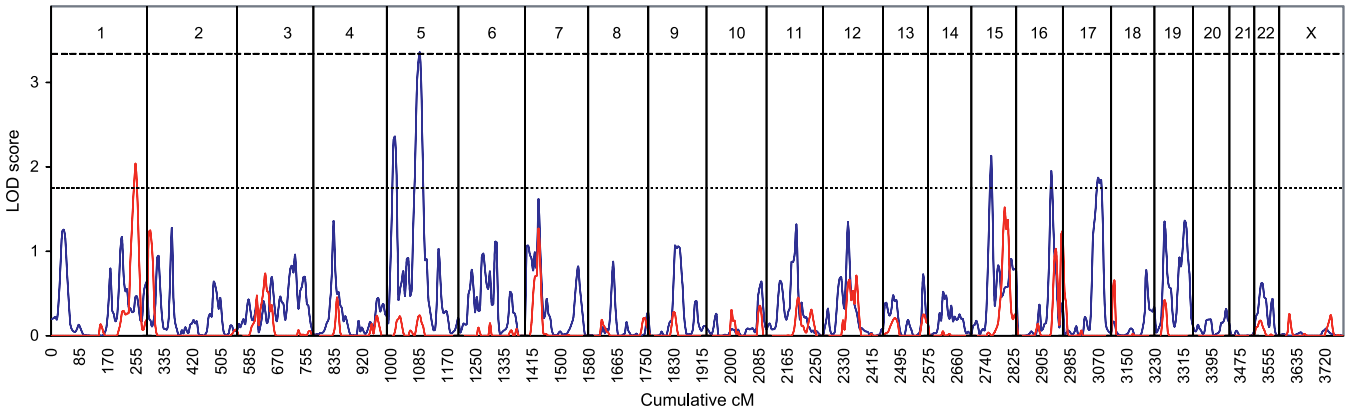

Figure 1. Results of Genome-Wide Univariate and Multivariate Linkage Analyses

Results of univariate (red line) and multivariate (blue line) linkage analyses for absolute finger ridge count, showing empirical significant (dashed line) and suggestive (dotted line) thresholds for the univariate analysis obtained via simulation (1,000 replicates)

doi:10.1371/journal.pgen.0030165.g001

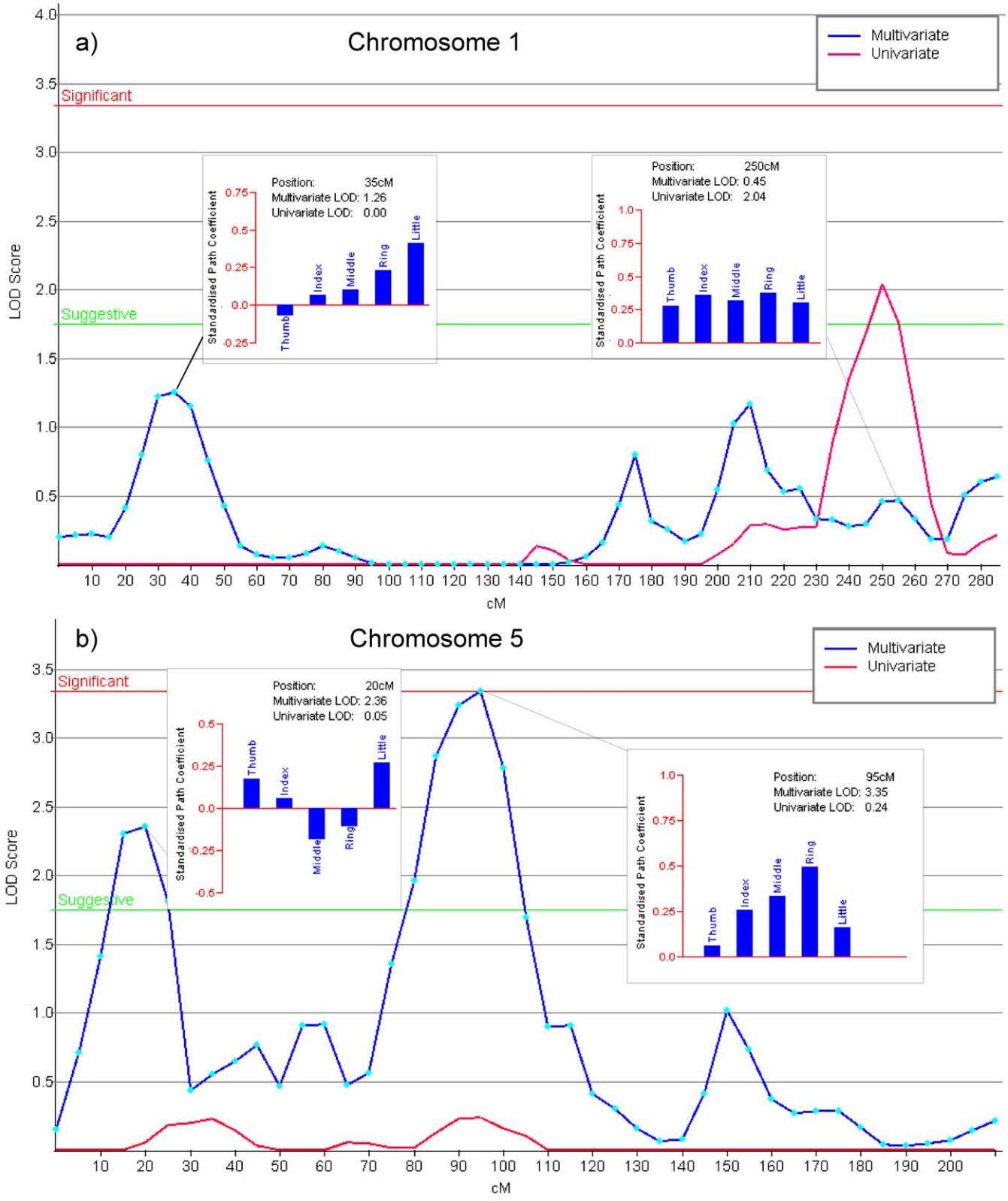

Figure 2. Results of Univariate (Red Line) and Multivariate (Blue Line) Linkage Analyses for Absolute Finger Ridge Count on Chromosomes 1 (A) and 5 (B).

Empirical significant (thin red line) and suggestive (green line) thresholds for the univariate analysis obtained via simulation (1,000 replicates). Light blue dots indicate the 5-cM intervals at which linkage analyses were conducted. The inset graphs show the standardized path coefficients from the QTL factor from the multivariate analysis for each of the fingers. (Note: squaring the standardized path coefficients yields an estimate of the proportion of variance for each digit explained by the QTL.)

doi:10.1371/journal.pgen.0030165.g002

Table 1. Linkage Regions Yielding LOD Scores over 1 (Bold), Change in Minus Twice Log-Likelihood (−2LL), LOD Scores the Standardized Path Coefficients (SPC) from the QTL Factors of the Univariate and Multivariate Genome Scans

Chromosome	Location cM	Univariate Results			Multivariate Results						
		$X^2_{0.1}$	LOD	QTL SPC	X^2_5	LOD	Standardized Path Coefficients				
							I (Thumb)	II (Index)	III (Middle)	IV (Ring)	V (Little)
Chromosome 1	35	.00	.00	.00	13.91	**1.26**	−.07	.06	.10	.23	.41
	210	1.31	.28	.34	13.31	**1.16**	.25	.36	.34	.47	.28
	250	9.39	**2.04**	.46	8.18	.46	.28	.36	.32	.37	.30
Chromosome 2	5	5.74	**1.25**	.46	5.51	.18	.22	.22	.29	.36	.32
	70	.00	.00	.00	14.00	**1.27**	.37	.01	−.06	.06	.16
Chromosome 4	55	.14	.03	.27	14.57	**1.36**	−.04	−.08	.02	.23	.36
Chromosome 5	20	.26	.06	.29	20.54	**2.36**	.17	.06	−.19	−.11	.27
	95	1.09	.24	.19	26.04	**3.34**	.06	.26	.34	.49	.16
Chromosome 7	5	.00	.00	.21	12.66	**1.07**	.19	.06	−.07	.02	.35
	35	5.83	**1.27**	.45	16.16	**1.62**	.34	.37	.28	.30	.44
Chromosome 9	85	.02	.00	.22	12.61	**1.06**	.26	.14	−.05	.03	.29
Chromosome 11	85	1.52	.33	.33	14.26	**1.31**	.04	.02	.26	.35	.12
Chromosome 12	70	2.85	.62	.41	14.49	**1.35**	.02	.22	.35	.42	.29
Chromosome 15	55	.00	.00	.26	19.17	**2.12**	−.09	.13	.16	.12	.39
	95	7.00	**1.52**	.45	9.06	.57	.06	.34	.25	.10	.16
Chromosome 16	100	.19	.04	.19	18.12	**1.94**	−.07	.12	.28	.27	.38
	130	5.46	**1.19**	.46	7.46	.38	.23	.39	.31	.31	.32
Chromosome 17	100	.00	.00	.00	17.68	**1.87**	.13	.12	−.22	−.11	.03
Chromosome 19	25	1.93	.42	.34	14.43	**1.34**	.27	.44	.32	.18	.20
	85	.00	.00	.00	14.57	**1.36**	.04	.16	.04	−.21	.11

doi:10.1371/journal.pgen.0030165.t001

fingers [6,8]. The QTL loading was strongest for the ring finger (24.1% of the variation), explained around 6.6% and 11.2% of variance in ridge counts on the index and middle fingers, respectively, 2.6% in little finger ridge count, and less than 1% in thumb ridge count. Post-hoc univariate linkage analyses for each finger individually (shown in Figure 3) confirmed this pattern of factor loadings. Pointwise simulations (described below) revealed that a LOD score this extreme arose by chance in 1/4,000 simulations, yielding a pointwise empirical *p*-value of 0.00025.

There was no evidence for linkage to the X chromosome. The highest LOD score observed (LOD = 0.25) was for the univariate analyses at a locus at 25 cM. It is possible that the assumption of dosage correction may have obscured linkage to a gene acting in a pseudoautosomal manner. However, a post-hoc univariate analysis (not shown here) of the total absolute ridge count, in which there was no assumption of dosage compensation, did not yield any further evidence for linkage.

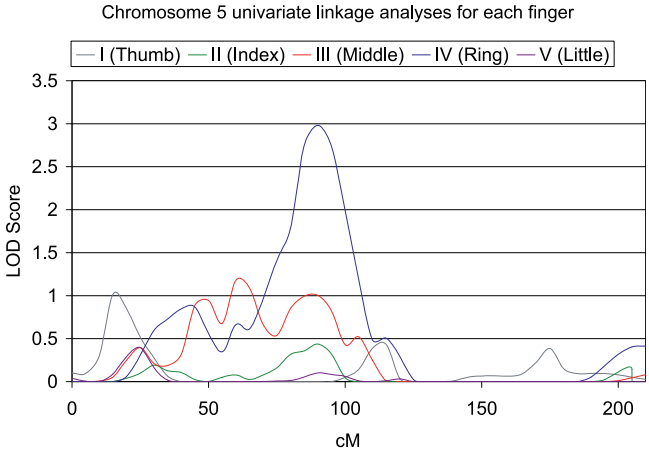

Figure 3. Univariate Variance Components Linkage Analyses for Individual Finger Ridge Count on Chromosome 5

doi:10.1371/journal.pgen.0030165.g003

Discussion

As this is the first linkage analysis for finger ridge count, these peaks are novel and there are numerous candidate genes lying under them that warrant investigation. The linkage region on Chromosome 5 contains a number of zinc-finger genes *(ZFYVE16, ZCCHC9,* and *ZBED3)*. Similarly, the peak on Chromosome 19 (85 cM) spans a cluster of zinc-finger genes. The Chromosome 15 (55 cM) peak is within 5 cM of the Fibrillin 1 gene *(FBN1)*, which is involved in maintenance of elastic fibers and anchoring epithelial cells to the interstitial matrix. Mutations in this gene result in severe developmental malformations of the hands (among other phenotypes) and are a major cause of Marfan syndrome and a range of other conditions that result in arachnodactyly or brachydactyly. Given findings that ridge count is correlated with finger length in a sample of individuals with Marfan syndrome [15], it seems plausible that polymorphic variations in this gene that influence the development of the digits may have a secondary influence on the normal development finger pads and dermal ridges.

Early studies attempted to link the presence of an arch pattern (i.e., a zero ridge count) on any finger to blood groups, finding no linkage to the rhesus (1p36.2–1p34) or P1 (22q13.2) blood groups but some evidence for linkage to the haptoglobin locus (16q22.1) [16]. The small peak in both the

Table 2. Genetic and Environmental Standardized Path Coefficients from the Multivariate (Null) Model in Which the QTL Factor Loadings Were Set to Zero

Coefficients	Hand	Finger	Factors									
			1	2	3	4	5	6	7	8	9	10
Additive genetic path coefficients	Left hand	I	.714									
		II	.783	.044								
		III	.686	−.031	.191							
		IV	.713	.090	.456	.015						
		V	.622	.407	.251	.031	.000					
	Right hand	I	.714									
		II	.783	.044								
		III	.686	−.031	.191							
		IV	.713	.090	.456	.015						
		V	.622	.407	.251	.031	.000					
Non-additive (dominant) genetic path coefficients	Left hand	I	.506									
		II	−.162	.402								
		III	−.136	.239	.447							
		IV	−.069	.129	.152	.248						
		V	.019	.136	.034	.127	.373					
	Right hand	I	.506									
		II	−.162	.402								
		III	−.136	.239	.447							
		IV	−.069	.129	.152	.248						
		V	.019	.136	.034	.127	.373					
Unique environmental (residual) path coefficients	Left hand	I	.485									
		II	.052	.441								
		III	.046	.081	.456							
		IV	.020	.023	.034	.408						
		V	.046	−.009	.019	.062	.449					
	Right hand	I	−.028	.031	.061	.052	.018	.476				
		II	.042	−.064	.008	.028	.004	.056	.433			
		III	−.010	−.029	−.029	−.022	.011	.058	−.010	.459		
		IV	−.075	−.034	−.005	−.008	−.008	.020	.022	−.024	.401	
		V	−.015	.030	−.007	.036	−.055	.057	.007	.026	.035	.444

Note that for additive and dominant factors, loadings are constrained equal for homologous digits on left and right hands.

doi:10.1371/journal.pgen.0030165.t002

univariate and multivariate genome scans on Chromosome 16 at 110 cM is approximately 15 cM distal to the haptoglobin locus, so it is possible that this peak may in fact replicate these early findings.

As evident from Table 1, a variety of factor loading patterns were observed during the multivariate genome scan. At the multivariate level, the genetic and environmental factor loadings (summarized in Table 2) showed patterns consistent with developmental fields, such as the peaks on Chromosome 5 (95 cM) and Chromosome 1 (35 cM), in which the covariation between adjacent fingers was higher than between more distal fingers. At other loci, such as the second highest multivariate linkage peak, on Chromosome 15 (55 cM), the peak loaded predominantly on a single pair of digits. These findings were anticipated by earlier multivariate genetic analyses of ridge counts that found evidence of both common and group (or field) genetic factors responsible for the high level of covariation between ridge counts on different digits, including some of the QTL factor patterns seen here [7].

Although the multivariate peak on Chromosome 5 was primarily driven by the fourth digit, it is unlikely that this result is a consequence of the missing data in the adult sample. The missing data from digits IV and V were not imputed, and may be considered missing completely at random (as the decision not to collect prints on digits IV and V was unrelated to the ridge counts that would have been observed) [17]. The analytic approach used in these analyses (raw continuous data maximum likelihood analyses implemented in Mx [18]) has previously been shown to yield unbiased results when the distribution in normal or slightly skewed and missing values are missing completely at random [19]. In addition, the post hoc univariate analyses (Figure 3; in which all available data for each digit were analyzed in separate univariate analyses) provide support for the multivariate results. As expected, the highest peak was observed for the 4th digit, followed by the 3rd and the 2nd.

The absence of significant univariate results and the general dearth of peaks from the univariate analysis of ARC suggest that the simple pleiotropic model specified by using a sum score such as ARC alone is not sufficient to characterize the rich biological interrelationships influencing finger ridge count. However, in some areas, such as the peak on Chromosome 1, we did observe QTL loadings that were consistent with pleiotropic effects. In addition, given the disparity between the digits in their contributions to the multivariate peak on Chromosome 5, assessing the individual contributions of the fingers may also provide information that can aid in the interpretation of multivariate linkages. These analyses have shown that even for conceptually and

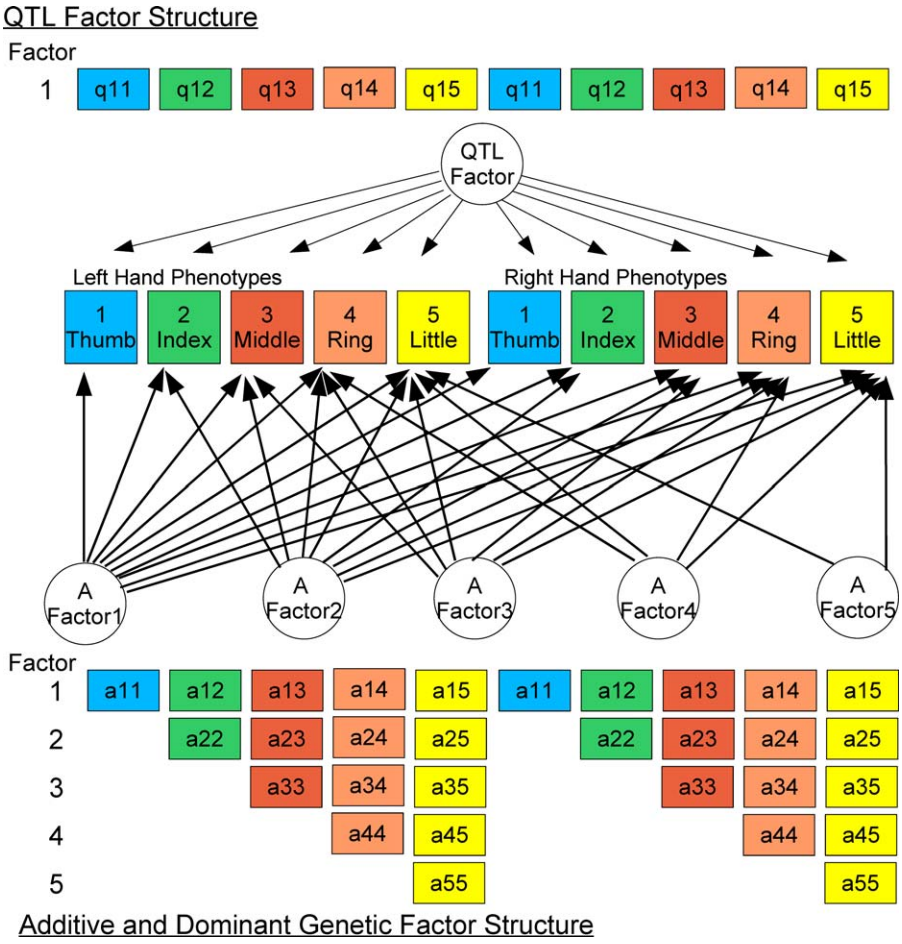

Figure 4. Schematic Representation of the Additive and Dominant Genetic and QTL Factor Structures

The unique environmental factors structure (not shown) contained ten variables (using a full Cholesky decomposition). In the diagram below, color coding is used to indicate which parameters load on each digit, while horizontal arrays are used to indicate factor structure (e.g., the first additive genetic factor loads on all ten phenotypes, while factor 5 loads only on the little finger).

doi:10.1371/journal.pgen.0030165.g004

theoretically simple phenotypes such as finger ridge count, using a single approach to linkage analyses (such as a sum score) may place biologically implausible restrictions upon the model, significantly reducing the power to detect effects and the interpretability of results.

A limitation of our study is the well-known low power of sib-pair linkage analysis for unselected samples, which can in part be ameliorated through multivariate analysis [14,20]. The apparent advantages of multivariate analysis revealed here are somewhat exaggerated by our inability to calculate the total ARC for adult twins because only digits I to III were counted in that study. However, as discussed above, using the raw data maximum likelihood option in Mx, joint analysis of the six fingers for which adult data are available, together with the almost complete adolescent set, increases power of the multivariate analysis by making use of every measured data point while providing estimates of factor loadings unbiased by missing values [17].

In conclusion, we report the first linkage scan for finger ridge count, finding a significant peak on Chromosome 5 and suggestive peaks on Chromosomes 1 and 15. Both pleiotropic QTL effects consistent with development fields and non-pleiotropic effects influencing single fingers were observed. In addition, we have demonstrated that a comprehensive approach involving both multivariate analyses of constituent phenotypes and univariate analyses of a sum score can be more informative than simple univariate analyses in the presence of complex pleiotropic models.

Materials and Methods

The data were collected within the context of an adolescent twin family study [11,12] and an adult twin study [13]. Characteristics of the phenotypic and genotypic data are provided in Table 3.

Phenotypic data. Rolled fingerprints were collected from twin pairs and their available siblings by research nurses trained to ensure that prints contained the centre of the pattern and all triradii. In the adult study, because of a shortage of time in the protocol, prints were only collected from the first three fingers of each hand (it is much harder and takes longer to obtain good prints of digits IV and V (the ring and little fingers) using traditional methods). From 1994 to 2005, prints were collected using a fingerprint ink pad and archival quality paper. From 2005 onwards, prints were collected using an electronic rolled fingerprint scanner (Smiths Heimann Biometrics ACCO1394, http://www.shb-jena.com/ACCO1394__scanner__AQ.pdf).

The majority of ridge counts analyzed here were scored from the inked prints and counted by eye using a binocular dissecting microscope (counting was performed by three of the authors, BM, DZL, and SEM). The number of ridges lying between the center of the pattern (core) and the triradius/triradii (delta) were counted using standard conventions [6]. Ridge counts for ten individuals were

Table 3. Characteristics of Participants, Genotypic, and Phenotypic Data

Characteristics			Adolescent Study		Adult Study	Combined Sample
			MZ Families	DZ Families	DZ Families	
Genotypic characteristics	*N* families		187	406	329	992
	N individuals		464	986	664	2114
	N sibships of size:	2	110[a]	269	326	705
		3	64	105	-	169
		4	10	30	3	43
		5	2	3	-	5
		N markers	203–756		227-1650	
		Mean (sd) markers	562.0 (185.4)		812.3 (287.5)	
		% Female	50%		61.7%	53.7%
Phenotypic characteristics[b]	Left hand absolute ridge counts: Mean (sd)	I (Thumb)	19.12 (10.64)		18.01 (10.40)	18.78 (10.58)
		II (Index)	13.83 (11.16)		13.30 (11.35)	13.67 (11.22)
		III (Middle)	12.99 (9.81)		12.91 (9.93)	12.97 (9.84)
		IV (Ring)	18.66 (10.88)		Not collected	18.66 (10.88)
		V (Little)	13.91 (6.88)		Not collected	13.91 (6.88)
	Right hand absolute ridge counts: Mean (sd)	I	23.17 (11.23)		21.67 (11.26)	22.7 (11.26)
		II	14.47 (11.62)		13.78 (11.91)	14.25 (11.72)
		III	12.85 (8.84)		12.56 (9.26)	12.76 (8.97)
		IV	19.98 (11.53)		Not collected	19.98 (11.53)
		V	14.36 (7.42)		Not collected	14.36 (7.42)
	Absolute ridge count (sum of all ten fingers): Mean (sd)		163.34 (78.64)		Incalculable	163.34 (78.64)

[a]These 110 MZ sib-pairs were included to allow the within family shared variance to be partitioned into that due to additive and dominant genetic effects. These pairs were assumed to be IBD2 across the genome; zygosity had been confirmed by genotyping nine highly polymorphic loci.
[b]Absolute ridge counts in this sample are comparable to those observed in other Caucasian samples [31]
DZ, dizygotic; MZ, monozygotic; sd, standard deviation.
doi:10.1371/journal.pgen.0030165.t003

scored from the electronic prints using a purpose-built software package [21] . Summary statistics are given in Table 3. Since ARC is calculated by summing the ridge counts of all ten fingers, it could not be calculated for individuals with missing data, including all the adult twins. The phenotypic correlations between digits and ARC are shown in Table 4. To improve computational efficiency phenotypes were corrected for mean differences between males and females, and transformed to *z*-scores prior to analysis.

Genotypic data. Genotypic data were available for 1,230 twins and sibs with fingerprint phenotypes from the adolescent and 664 twin individuals from the adult study (as detailed in Table 3). In addition, 110 nongenotyped monozygotic pairs from the adolescent study were included in these analyses to allow the within-family shared variance to be partitioned into that due to additive and dominant genetic effects, respectively [22]. The cleaning and error checking of the genotypic data for the adolescent and adult studies have been described in detail elsewhere [23,24]. In summary, the adolescent genotypic data was composed of three waves of genotyping. Each wave of genotyping included overlapping samples and markers in order to check data quality. Following error checking and data cleaning [24], the resulting genotypic dataset comprised 796 markers (35 of which are duplicates) at an average spacing of 4.8 cM (Kosambi). Similarly, the adult genotypic data was composed of four waves of genotyping, with duplicate individuals and markers between each wave of genotyping. Following error checking and data cleaning [23], the resulting genotypic dataset comprised a dense map of 1770 markers (394 of which are duplicates) at an average spacing of 6.1 cM (Kosambi). Since the adolescent and adult marker sets only partly overlapped, Identity By Descent (IBD) estimates and information contents were obtained separately for the two samples using a standard map[25] at 5cM intervals across the genome using MERLIN 1.0.1[26]. As the IBD estimates were made at fixed points along the

Table 4. Phenotypic Correlations between Absolute Ridge Count on Each Digit, Correlations between Homologous Digits in Bold

Digits	Left Hand					Right Hand				
	I	II	III	IV	V	I	II	III	IV	V
Left hand II	.51									
Left hand III	.44	.70								
Left hand IV	.47	.63	.69							
Left hand V	.47	.55	.51	.67						
Right hand I	**.76**	.50	.46	.51	.49					
Right hand II	.49	**.78**	.66	.63	.55	.50				
Right hand III	.41	.64	**.76**	.66	.50	.45	.65			
Right hand IV	.42	.60	.66	**.82**	.64	.50	.62	.66		
Right hand V	.44	.56	.49	.66	**.77**	.51	.55	.51	.67	
Total absolute ridge count	.69	.83	.81	.86	.76	.72	.82	.78	.84	.76

doi:10.1371/journal.pgen.0030165.t004

chromosomes, the data from the two samples could then be jointly modeled at 5-cM intervals. Characteristics of these participants and the genotypic information available are summarized in Table 3.

Analytic methods. All linkage analyses were conducted by variance components analysis using raw data maximum likelihood methods implemented in Mx1.63 [18]. For the autosomal univariate variance components QTL analysis of ARC, a likelihood ratio chi-square test ($\chi^2_{0,1}$) was used to compare the fit of the alternate model, in which the total variance was modeled as the sum of the additive genetic, dominant genetic, QTL, and unique environmental variances ($H1 : \sigma^2_P = \sigma^2_A + \sigma^2_D + \sigma^2_Q + \sigma^2_E$) to a null model in which variance due to the QTL was set to zero ($H0 : \sigma^2_P = \sigma^2_A + \sigma^2_D + \sigma^2_E$).

Significant and suggestive thresholds and genome-wide empirical *p*-values were obtained by simulation. Data for 1,000 simulated unlinked genome scans that preserved the pedigree structures, information content, and missing data patterns were obtained using MERLIN–simulate [26]. IBDs were extracted from the simulated data, each replicate was analyzed in the same way as the observed data, and the highest LOD score for each chromosome was recorded. Empirical significant and suggestive thresholds were then estimated by extracting the LOD scores that were obtained with a probability of 0.05 (i.e., once in every 20 null replicates) and once per genome scan, respectively. Pointwise empirical *p*-values were obtained by calculating how often a result as extreme as that which was observed, for the given map position, occurred by chance within the simulated data. Genomewide empirical *p*-values were obtained by extracting the highest LOD score from each simulation replicate and recording how often a result as extreme as that which was observed occurred by chance within these simulated data.

For the autosomal multivariate analysis of individual finger ridge counts, use of raw data within Mx analyses allowed the inclusion of individuals with missing data (in particular, all the adults twins missing prints for digits IV and V). A similar alternate model was used ($H1 : \sigma^2_P = \sigma^2_A + \sigma^2_D + \sigma^2_Q + \sigma^2_E$). To provide the most conservative test of QTL variance, saturated factor models were fitted for A, D, and E components, with the constraint for A and D matrices that the factor loadings, patterned as a 5×5 Cholesky decomposition, be equal for corresponding fingers on left and right hands. In this way, we sought to capture the major QTL features while minimizing capitalization on chance. As summarized in Figure 4, the alternate model thus contained five additive genetic factors, five dominant genetic factors, a single QTL factor, and ten unique environmental factors (patterned as a full 10×10 Cholesky decomposition). The single QTL factor influenced all phenotypes and contained five estimated parameters, one for each of the five pairs of digits. In the null model ($H0 : \sigma^2_P = \sigma^2_A + \sigma^2_D + \sigma^2_E$), the QTL factor loadings were set to zero. A likelihood ratio chi-square test with five degrees of freedom (χ^2_5)was used to test the difference in fit of these two models. To obtain LOD score equivalents for this test, χ^2_5 was converted to a *p*-value, which was then transformed to a standard LOD score. Given the time required to conduct the multivariate linkage analysis (over an hour per marker on our Linux server), calculation of empirical significance values was not feasible. Instead, a pointwise empirical *p*-value was calculated at the highest peak using simulated IBD data information derived from ped files made using MERLIN–simulate (4,000 replicates).

For X chromosome linkage analyses, we implemented a simple extension of the X-linked variance components model [27], in which an extra additive genetic variance component is modeled with the coefficient of relatedness (usually set to 1/2 in the autosomal case) corrected for the sexes of the siblings for each sib-pair combination. As for the autosomal additive polygenetic case, covariation among relatives due to additive X-linked variance arises because of alleles shared IBD. Assuming complete random X-inactivation (lyonization), then ψ_{ij}, the coefficient of X-chromosome relationship [28] was set to 1/2 for brother–brother pairs, 3/8 for sister–sister pairs, and 1/4 for opposite-sex pairs. In the multivariate analyses, the additional X-linked additive genetic variance component was patterned as a 5×5 Cholesky decomposition, with parameters constrained to be equal for corresponding fingers on left and right hands. As for the autosomal case, in the multivariate analyses a single QTL factor was modeled that loaded on all phenotypes and contained five estimated parameters, one for each of the five pairs of digits. The QTL model also assumed complete random X-inactivation, so that the X-linked QTL variance in females was set to be half that of males. Following the suggestion of Kent et al. [29,30], separate unique environmental effects were estimated for males and females to allow for genotype or environment interactions with sex. Based on the results of these analyses, a post hoc decision was made not to obtain empirical *p*-values for these X-linked analyses.

Supporting Information

Accession Numbers

The National Center for Biotechnology Information (NCBI) Online Mendelian Inheritance in Man (OMIM) database (http://www.ncbi.nlm.nih.gov/sites/entrez?db=OMIM) accession numbers for the syndromes discussed in this paper are: Marfan syndrome, #154700 and Dermatoglyphics—arch on any digit, 125570.

The NCBI OMIM database accession numbers for the genes discussed in this paper are Fibrillin 1 *(FBN1),* *134797; Haptoglobin blood group, *140100; P1 blood group, #111400; and Rhesus blood group, +111700.

The NCBI Entrez (http://www.ncbi.nlm.nih.gov/sites/gquery) database accession numbers for the genes discussed in this paper are *ZBED3*, 84327; *ZCCHC9*, 84240; and *ZFYVE16*, 9765.

Acknowledgments

The authors would like to thank the twins and their families for their participation. For the ongoing data collection, recruitment, and organization of the studies in which the phenotypes were collected, the authors wish to thank Marlene Grace and Ann Eldridge (who collected the majority of the fingerprints); Alison Mackenzie and Amanda Baxter (for daily management of the study) and Margie Wright for supervision; and Daniel Park for writing the program used to obtain the semiautomatic ridge counts. The genome scans of adolescents were supported by the Australian National Health and Medical Research Council's Program in Medical Genomics (NHMRC-219178) and a grant to Jeff Trent from the Center for Inherited Disease Research (CIDR) at Johns Hopkins University. CIDR is fully funded through a federal contract from the National Institutes of Health to The Johns Hopkins University, Contract Number N01-HG-65403. For genome scans of adults, we acknowledge and thank the Mammalian Genotyping Service, Marshfield, Wisconsin (Director James Weber) for genotyping under grants to Daniel T. O'Connor, David Duffy, Patrick Sullivan, and Dale Nyholt; Aarno Palotie and Leena Peltonen for the Helsinki genome scan (under the GenomEUtwin project which is supported by the European Union contract number QLRT-2001–01254); Eline Slagboom, Bas Heijmans, and Dorret Boomsma for the Leiden genome scan; Peter Reed for the Gemini genome scan; and Jeff Hall for the Sequana genome scan.

Author contributions. SEM and NGM conceived and designed the experiments. SEM analyzed the data and wrote the paper. GWM contributed reagents/materials/analysis tools. DZL and BM provided methodological support in the collection of phenotypic data and performed ridge counts. GZ provided analytical advice and cleaned the genotypic data. NGM provided analytical advice and assisted in the writing of the manuscript

Funding. This research was supported in part by grants from NIAAA (USA) AA007535, AA013320, AA013326, AA014041, AA07728, AA10249, AA11998, and NHMRC (Australia) 941177, 951023, 950998, 981339, 241916, and 941944. SEM is supported by NHMRC (Australia) Sidney Sax Fellowship 443036.

Competing interests. The authors have declared that no competing interests exis

References

1. Bonnevie K (1924) Studies on papillary patterns of human fingers. J Genet 15: 1–111.
2. Johnson KO (2001) The roles and functions of cutaneous mechanoreceptors. Curr Opin Neurobiol 11: 455–461.
3. Loesch DZ, Lafranchi M, Ruffolo C (1990) Hand locomotor functions, body structure, and epidermal ridge patterns: preliminary study. Hum Biol 62: 665–679.
4. Wheat HE, Goodwin AW (2000) Tactile discrimination of gaps by slowly adapting afferents: effects of population parameters and anisotropy in the fingerpad. J Neurophysiol 84: 1430–1444.
5. Loesch DZ (1983) Quantitative dermatoglyphics: classification, genetics, pathology. Oxford: Oxford University Press. 450 p.
6. Holt SB (1968) The genetics of dermal ridges. Springfield: Charles C Thomas. 400 p.
7. Martin NG, Eaves LJ, Loesch DZ (1982) A genetical analysis of covariation between finger ridge counts. Ann Hum Biol 9: 539–552.
8. Loesch DZ, Huggins RM (1992) Fixed and random effects in the variation of

the finger ridge count: a study of fragile-X families. Am J Hum Genet 50: 1067–1076.
9. Spence MA, Elston RC, Namboodiri KK, Pollitzer WS (1973) Evidence for a possible major gene effect in absolute finger ridge count. Hum Hered 23: 414–421.
10. Spence MA, Westlake J, Lange K (1977) Estimation of the variance components for dermal ridge count. Ann Hum Genet 41: 111–115.
11. Wright M, De Geus E, Ando J, Luciano M, Posthuma D, et al. (2001) Genetics of cognition: outline of a collaborative twin study. Twin Res 4: 48–56.
12. Wright MJ, Martin N (2004) Brisbane adolescent twin study: outline of study methods and research projects. Aust J Psychol 56: 65–78.
13. Heath AC, Bucholz KK, Madden PA, Dinwiddie SH, Slutske WS, et al. (1997) Genetic and environmental contributions to alcohol dependence risk in a national twin sample: consistency of findings in women and men. Psychol Med 27: 1381–1396.
14. Martin N, Boomsma D, Machin G (1997) A twin-pronged attack on complex traits. Nat Genet 17: 387–392.
15. Mglinets VA, Rudaeva AI (1991) [Relationship between finger length and ridge count in patients with Marfan syndrome]. Genetika 27: 1984–1993.
16. Anderson MW, Bonne-Tamir B, Carmelli D, Thompson EA (1979) Linkage analysis and the inheritance of arches in a Habbanite isolate. Am J Hum Genet 31: 620–629.
17. Little R, Rubin D (1987) Statistical analysis with missing data. New York: Wiley and Son. 408 p.
18. Neale MC, Boker SM, Xie G, Maes HH (2006) Mx: statistical modeling. Richmond (Virginia): Virginia Commonwealth University Department of Psychiatry. Available: http://www.vcu.edu/mx/. Accessed 1 September 2007. 204 p.
19. Graham J, Hofer S, MacKinnon D (1996) Maximizing the usefulness of data obtained with planned missing value patterns: An application of maximum likelihood procedures. Multivariate Behav Res 31: 197–218.
20. Eaves LJ, Neale MC, Maes H (1996) Multivariate multipoint linkage analysis of quantitative trait loci. Behav Genet 26: 519–525.
21. Medland SE, Park DA, Loesch DZ, Martin NG (2007) Ridgecounter: a program for obtaining semi-automated finger ridge counts. Ann Hum Biol 34: 504–517.
22. Evans DM, Medland SE (2003) A note on including phenotypic information from monozygotic twins in variance components QTL linkage analysis. Ann Hum Genet 67: 613–617.
23. Cornes BK, Medland SE, Ferreira MA, Morley KI, Duffy DL, et al. (2005) Sex-limited genome-wide linkage scan for body mass index in an unselected sample of 933 Australian twin families. Twin Res Hum Genet 8: 616–632.
24. Zhu G, Evans DM, Duffy DL, Montgomery GW, Medland SE, et al. (2004) A genome scan for eye colour in 502 twin families: most variation is due to a QTL on chromosome 15q. Twin Res 7: 197–210.
25. Duffy DL (2006) An integrated genetic map for linkage analysis. Behav Genet 36: 4–6.
26. Abecasis GR, Cherny SS, Cookson WO, Cardon LR (2002) Merlin–rapid analysis of dense genetic maps using sparse gene flow trees. Nat Genet 30: 97–101.
27. Jardine R, Martin N (1984) No evidence for sex-linked or sex-limited gene expression influencing spatial orientation. Behav Genet 14: 345–354.
28. Ekstrom CT (2004) Multipoint linakge analysis of quantitative traits on sex-chromosomes. Genet Epidemiol 26: 218–230.
29. Kent JW, Dyer TD, Blangero J (2005) Estimating the additive genetic effect of the X chromosome. Genet Epidemiol 29: 377–388.
30. Kent JW Jr., Lease LR, Mahaney MC, Dyer TD, Almasy L, et al. (2005) X chromosome effects and their interactions with mitochondrial effects. BMC Genetics 6 Suppl 1: S157.
31. Greally MG, Roberts DF (1991) A study of digital dermatoglyphics in Ireland. Ann Hum Biol 18: 485–496.